J Fluoresc (2009) 19:267–275
DOI 10.1007/s10895-008-0412-4

ORIGINAL PAPER

Binding Properties of Water-Soluble Carbosilane Dendrimers

Elzbieta Pedziwiatr · Dzmitry Shcharbin · Louis Chonco · Paula Ortega · F. Javier de la Mata · Rafael Gómez · Barbara Klajnert · Maria Bryszewska · Ma Angeles Muñoz-Fernandez

Received: 29 May 2008 / Accepted: 11 August 2008 / Published online: 30 August 2008

Abstract Dendrimers have been proposed as new carriers for drug delivery. They have distinctive characteristics, such as uniform and controlled size, monodispersity and modifiable surface group functionality, which make them extremely useful for biomedical applications. In this study, the binding capacity of water-soluble carbosilane dendrimers was examined. A double fluorimetric titration method with 1-anilinonaphthalene-8-sulphonic acid (ANS) was used to estimate the binding constant and the number of binding centers per dendrimer molecule. The data obtained suggest that ANS interacts non-covalently with the dendrimers. Second generation dendrimers have an open, asymmetric structure that allows them to encapsulate ANS. The ability of the polymers to interact with DNA was assessed by an ethidium bromide (EB) displacement assay. All the dendrimers studied bound to DNA in competition with EB, though the strength of binding varied. Dendrimer interactions with a protein (BSA) were tested using fluorescence quenchers. The dendrimers caused no conformation change in the protein, indicating that interactions between carbosilane dendrimers and BSA are weak and occur preferentially at the protein surface.

Keywords Carbosilane dendrimer · Drug delivery · Fluorimetric titration · EB intercalation · Fluorescence quenching

E. Pedziwiatr · D. Shcharbin · B. Klajnert · M. Bryszewska (✉)
Department of General Biophysics, University of Lodz,
12/16 Banacha St.,
90-237 Lodz, Poland
e-mail: marbrys@biol.uni.lodz.pl

L. Chonco · M. A. Muñoz-Fernandez
Laboratorio de Inmunobiología Molecular,
Hospital General Universitario Gregorio Marañón,
Madrid, Spain

P. Ortega · F. Javier de la Mata · R. Gómez
Departamento de Química Inorgánica, Universidad de Alcalá,
Campus Universitario,
Alcalá de Henares, Spain

L. Chonco · P. Ortega · F. Javier de la Mata · R. Gómez · M. A. Muñoz-Fernandez
Networking Research Center on Bioengineering,
Biomaterials and Nanomedicine (CIBER-BBN),
Barcelona, Spain

Introduction

There is a continual search for novel therapeutic strategies to improve the treatments of different diseases. In recent decades, studies of polymer chemistry in relation to biomedical sciences have led to the birth of nano-sized (5–100 nm) polymer-based pharmaceuticals. This family of constructs, termed polymer therapeutics, nanospheres, nanocontainers or nanodevices, is very promising in biomedical applications such as drug delivery, gene transfection and imaging [1]. Constructs used as carriers for drug delivery should generally be in the nanometer range and uniform in size so that their ability to cross cell membranes is enhanced and the risk of undesired clearance from the body through the liver or spleen is reduced [2]. The synthesis of dendrimers offers the opportunity to generate monodisperse, structure-controlled macromolecular architectures similar to those observed in biological systems [3–5]. Dendrimers may be visualized as consisting of three critical architectural domains: (a) a multivalent surface, containing a large number of potentially reactive/passive sites (nano-scaffolding); (b) an interior shell surrounding the core; and (c) a core to which the dendrons are attached [2]. The conformation of a dendrimer depends on the

solvent. Polar dendrimers have higher core densities in apolar solvents because the dendrimer arms are folded back into the interior, but have higher surface densities in polar solvents [6]. Less polar dendrimers (containing aryl groups or other hydrophobic units) show the opposite dependence of conformation on solvent and behave as inverse micelles [7].

There have been several thousand publications on the characterization of dendrimers, deploying a range of techniques including NMR, IR, Raman, UV-Visible and fluorescence spectrometry, circular dichroism, X-ray diffraction, mass spectrometry, SAXS, SANS, laser light scattering, microscopy, SEC, EPR, electrochemistry, electrophoresis, intrinsic viscosity, DSC and dielectric spectroscopy [8]. There are several different kinds of dendrimers, for example polyamidoamine (PAMAM), polypropyleneimine (PPI), polylysine (Ply), polybenzylether (PBzE), polyphenylene (PHEN), thiophosphoryl phenoxymethyl (methylhydrazono; PMMH). In recent years, much effort has been devoted to the preparation of dendrimers that are designed to be highly biocompatible and water-soluble. In addition, some dendrimers have been designed to be biodegradable, with monomer units that are intermediates or products of metabolic pathways [9]. Some dendrimers have different biofunctional moieties, for example folic acid [10] and polyethylene oxide chains (PEO) [11].

Comparison of the features of dendrimers with those of linear polymers shows that the dendritic architecture provides several advantages for drug delivery applications. For example, the controlled multivalency allows several drug molecules, targeting groups and solubilizing groups to be attached in a well-defined manner to the periphery of a dendrimer. In addition, the low polydispersity should provide more reproducible pharmacokinetic behavior than is obtained using linear polymers that contain fractions with vastly different molecular weights. Furthermore, the relatively globular shapes of dendrimers, as opposed to the random coil structure of most linear polymers, could affect their biological properties, leading to interesting effects related to macromolecular architecture [9].

Early studies of dendrimers as potential delivery systems focused on their use as unimolecular micelles and boxes for the noncovalent encapsulation of drug molecules [12–15].

An alternative approach to the development of dendrimers as drug carriers is to exploit their well-defined multivalency by attaching drug molecules covalently to the periphery. Drug loading can be tuned by varying the generation number of the dendrimer, and drug release can be controlled by incorporating degradable drug-dendrimer linkages. Yang and Lopina have conjugated penicillin V with G2.5 and G3 PAMAM [16] and the antidepressant venlafaxine with G2.5 PAMAM [17]. Several workers have developed dendrimer conjugates with potential application as vehicles for delivering anticancer agents such as cisplatin [18], doxorubicin [19], methotrexate [20] and 5-fluorouracil [21].

The large numbers of ionizable groups on dendrimer surfaces present an interesting opportunity to attach numerous ionizable drugs electrostatically, enhancing water solubility. Also, the interiors of several dendrimer classes are available for complexing with ions [22]. Cationic dendrimers with primary amine end groups ($–NH_2$) on the surface and tertiary amine groups (>N–) at branching points in the core can interact with anionic groups of polymer chains, i.e. they can be fully penetrated by linear polyanions [23]. In contrast, linear polycations can only interact with carboxylated dendrimers via the dendrimer surface groups, possibly because the tertiary amine groups in the dendrimer core restrict penetration by the polycation [24]. Cationic dendrimers have been complexed with ibuprofen [25], piroxicam [26] and indomethacin [27], and also with DNA or oligonucleotides. Electrostatic interactions between dendrimers and anionic genetic material have been widely studied during recent years and open the possibility of using dendrimers for gene transfection.

The aim of this study was to characterize the binding properties of water-soluble carbosilane dendrimers as candidates for drug targeting. For this purpose we have checked the ability of carbosilane dendrimers to bind ANS and DNA and their interactions with bovine serum albumin.

Water-soluble carbosilane dendrimers containing peripheral ammonium or amine groups have recently been described by our groups as biocompatible molecules with potential as non-viral carriers (low toxicity profiles, no antigenicity) [28, 29]. We previously showed that such dendrimers form complexes (dendriplexes) with oligonucleotides. The efficiency of formation and the stability of the dendriplexes depend on electrostatic interactions with the oligonucleotides. Dendriplex formation significantly decreases the interactions between oligonucleotides and albumin [30, 31]. To screen the dendrimers, however, more simple tests are needed in order to determine their binding capacity and their ability to interact with proteins. A double fluorometric titration technique involving intercalation of the fluorescent probe ANS and ethidium bromide (EB) allows us to study the binding properties of carbosilane dendrimers. Interactions with proteins were tested using fluorescence quenchers. The accessibility of the protein–dendrimer complex to quenchers allows such interactions to be estimated.

Materials and methods

Calf thymus DNA (ctDNA), ethidium bromide (EB), 1-anilinonaphthalene-8-sulphonic acid (ANS), bovine serum albumin (BSA), acrylamide, cesium chloride and potassium

iodide were obtained from Sigma-Aldrich (USA). Other chemicals were of analytical grade. Double-distilled water was used to prepare all solutions; 0.15 mol/l Na-phosphate buffer (pH 7.4) was used.

All fluorescence measurements were taken with a Perkin-Elmer LS-50B spectrofluorimeter at 37°C.

Dendrimer synthesis

The dendrimers used in this study were cationic carbosilane dendrimers with peripheral ammonium groups. They were prepared according by reported methods [28, 29]. These dendrimers were 2G-[Si(OCH_2-$CH_2NMe_3^+I^-$)]8 (**1**), 2G-[Si($OCH_2CH_2NMe_3^+I^-)_2$]8 (**2**), 2G-[Si{$O(CH_2)_2N(Me)(CH_2)_2NMe_3^+I^-$}]8 (**3**) and 2G-[Si{$O(CH_2)_2N(Me)_2^+(CH_2)_2NMe_3^+(I^-)_2$}]8 (**4**). The abbreviation 2G means second generation. We have adopted the convention that each generation is formed on the basis of shell of silicon atoms. Then, starting from the core, this will be generation zero. The following four silicon atoms form the generation 1, and finally the eight terminal silicon atoms form the generation 2. This is independently of the number of terminal groups. We can have a second generation with eight or 16 groups. They contain one nitrogen atom (N) per branch (dendrimers **1**, **2**, called N group dendrimers) or two nitrogens (NN) per branch (dendrimers **3**, **4**, called NN group dendrimers). See Fig. 1 for molecular structures.

Double fluorimetric titration assay by ANS

ANS was dissolved in phosphate buffer. The excitation and emission wavelengths were set at 370 nm and between 400 and 600 nm respectively. It was established that the dendrimers alone were not excited by 370 nm irradiation and did not emit fluorescence. The excitation and emission slit widths were 5 and 2.5 nm, respectively. During measurements the samples were continuously stirred in 1-cm path length quartz cuvettes.

The binding constant (K_b) and the number of binding sites per dendrimer molecule (n) were estimated using double fluorimetric titration [32]. In the first fluorimetric titration, increasing concentrations of dendrimer were added to ANS solution at constant concentration and the maximum intensity (F_{max}) of ANS fluorescence was recorded. This corresponded to the binding of all the ANS molecules by the dendrimer. The maximum fluorescence

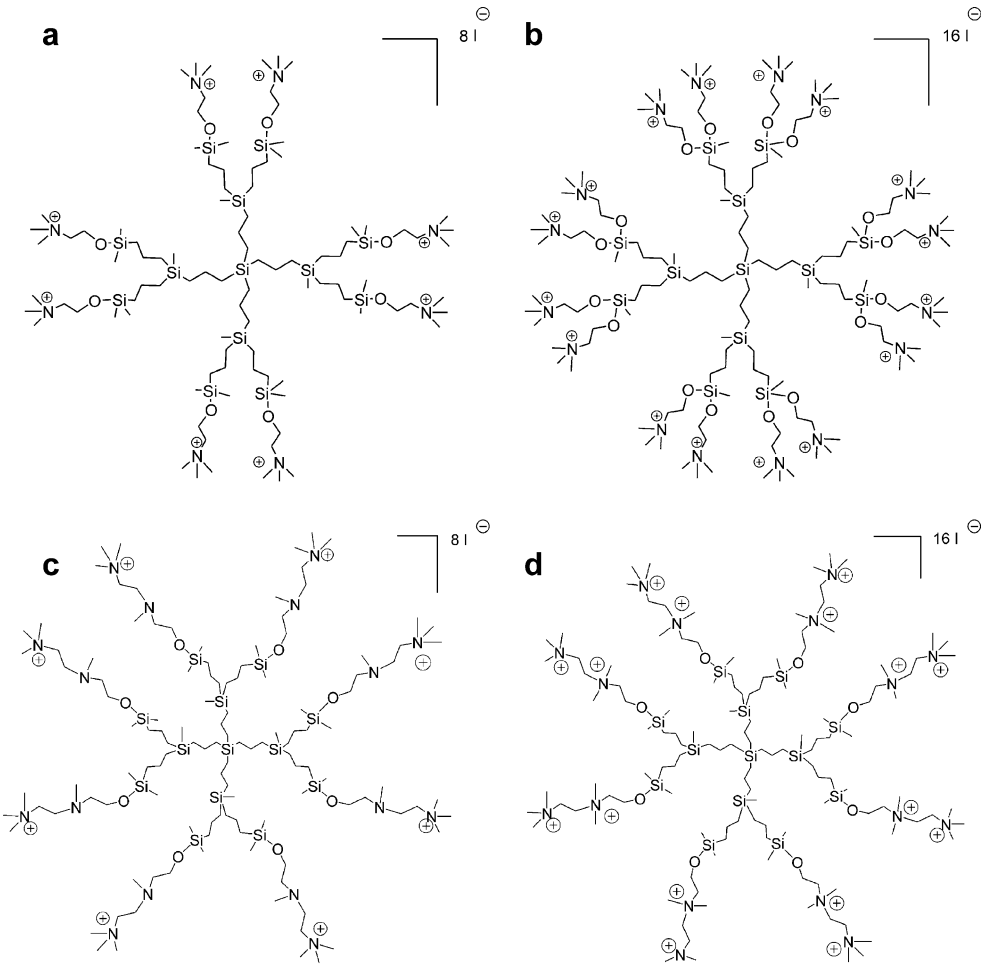

Fig. 1 The molecular structure of the dendrimers

intensity of ANS divided by its concentration gave the specific fluorescence intensity for the bound probe (F_{sp}):

$$F_{sp} = \frac{F_{max}}{C^1_{ANS}}, \quad (1)$$

where (C^1_{ANS}) is the ANS concentration during the first fluorimetric titration.

In the second titration, the dendrimer concentration (C_D) was constant while the ANS concentration was increased (C^2_{ANS}). The fluorescence intensity (F) was then measured. The concentration of ANS bound by dendrimers was calculated using the equation:

$$C^{bound}_{ANS} = \frac{F}{F_{sp}}, \quad (2)$$

The concentration of free ANS molecules was determined as follows:

$$C^{free}_{ANS} = C^2_{ANS} - C^{bound}_{ANS}. \quad (3)$$

The binding constants for the fluorescent probe molecules (K_b) and the number of ANS binding centers in the solution (N) could be can be calculated using the formula:

$$\frac{1}{C^{bound}_{ANS}} = \frac{1}{K_b \cdot N \cdot C^{free}_{ANS}} + \frac{1}{N}, \quad (4)$$

Equation 4 was modified by replacing the number of binding centers in solution (N) with the number of binding centers per dendrimer molecule (n), yielding the final equation:

$$\frac{C_D}{C^{bound}_{ANS}} = \frac{1}{K_b \cdot n \cdot C^{free}_{ANS}} + \frac{1}{n}, \quad (5)$$

where

$$n = \frac{N}{C_D} \quad (6)$$

and the constants were determined from the initial (linear) portions of a graph of $\frac{C_D}{C^{bound}_{ANS}}$ versus $\frac{1}{C^{free}_{ANS}}$ (Fig. 1c).

Ethidium bromide intercalation assay

Ethidium bromide and ctDNA were used at final concentrations of 1 μg/ml and 3 μg/ml, respectively, in 0.15 mol/l Na-phosphate buffer, pH 7.4. The fluorescence spectra of pure EB and of EB in the presence of DNA were recorded before and after addition of dendrimers. An excitation wavelength of 477 nm was used. The emission spectra were recorded from 500 to 800 nm. Under these conditions the fluorescence intensity of pure EB at the emission maximum (618 nm) was ~100 relative units of the device. The fluorescence intensity of EB in the presence of DNA before and after the dendrimers were added was measured at 604 nm (the emission maximum). The excitation and emission slit widths were set to 14.0 and 8.0 nm, respectively. The samples were contained in 1 cm path length quartz cuvettes and were continuously stirred. Before the fluorescent properties of the DNA–EB–dendrimer complex were examined, it was established that the dendrimers do not interact with EB.

The data were used to calculate the apparent dendrimer–ctDNA binding (association) constants (K^{DEN}_{ass}) using two different equations. The first equation is

$$K^{DEN}_{ass} = K^{EB}_{ass} \cdot \frac{[EB]_0}{[D]_{50}} \quad (7)$$

where K^{EB}_{ass} is the association constant of EB with ctDNA, $[EB]_0$ is the total concentration of EB in solution and $[D]_{50}$ is the concentration that generates a 50% decrease in the initial fluorescence intensity of the EB–DNA complex [33]. The second equation is

$$\frac{1}{K^I_{ass}} = \frac{IC_{50}}{1 + L_T \cdot K^L_{ass}} \quad (8)$$

where K^I_{ass} is the inhibitor association constant ($= K^{DEN}_{ass}$), IC_{50} is the concentration of inhibitor (I=dendrimer) necessary to displace 50% of the labeled ligand, L_T is the total concentration of the labeled ligand (EB) and K^L_{ass} is the association constant for the labeled ligand ($= K^{EB}_{ass}$) [34, 35].

It follows from these equations that

$$[D]_{50} = IC_{50} \quad (9)$$

In 0.2 mol/l Na-phosphate buffer (pH 7.4), $K^{EB}_{ass}$was $(1.70 \pm 0.04) \times 10^5$ $(mol/l)^{-1}$ [36].

To calculate the constants, the data graphs were modified so that the changes in fluorescence intensity of the EB–ctDNA complex when dendrimers were added were presented as

$$F^{rev} = \frac{F^{complex} - F^{pureEB}}{F^{complex}_0 - F^{pureEB}} \quad (10)$$

where $F^{complex}$ is the fluorescence of EB–ctDNA in the absence and presence of dendrimer, F^{pureEB} is the fluorescence of pure (free) EB, and $F^{complex}_0$ is the fluorescence of the EB–ctDNA complex in the absence of dendrimer when EB is fully bound by the ctDNA.

Fluorescence quenching

BSA was dissolved in 0.15 mol/l Na-phosphate buffer (pH 7.4) at 5 μmol/l. A neutral fluorescence quencher, acrylamide, and two ionic quenchers, potassium iodide (quenching ion I^-) and cesium chloride (quenching ion Cs^+), were used for these studies. Increasing aliquots of the quencher were added to 5 μmol/l BSA from a stock solution in water. The stock solutions of acrylamide, KI and CsCl were 1, 5 and 10 mol/l, respectively. The stock KI

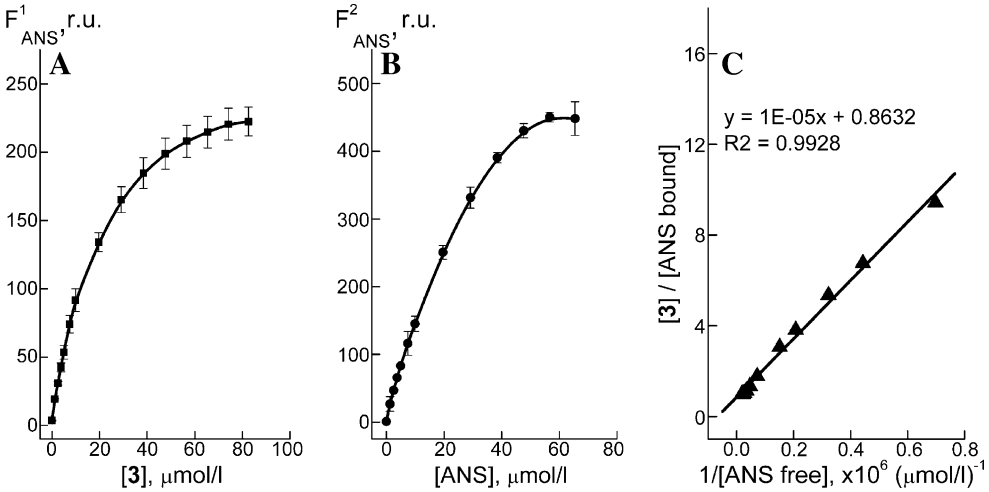

Fig. 2 Double fluorimetric titration of ANS vs dendrimer **3**: **a** The dependence of ANS fluorescence intensity on the concentration of dendrimer **3** at constant ANS concentration (5 μmol/l). **b** The dependence of ANS fluorescence intensity on ANS concentration at constant concentration of dendrimer **3** (10 μmol/l). **c** Scatchard–Klotz plot of [3]/[ANS bound] vs 1/[ANS free]. $\lambda_{exc.}$=370 nm, $\lambda_{em.}$=480 nm

solution contained 0.1 mmol/l $Na_2S_2O_3$ to prevent oxidation of I^- to I_3^-. The fluorescence intensity at the emission maximum (350 nm) was measured after excitation at 295 nm. The emission slit width was kept at 10 nm and the excitation slit width was 3.4 nm. Quenching data were collected for native BSA dissolved in buffer and for BSA supplemented with 0.1 mmol/l dendrimers.

The quenching results for acrylamide were analyzed by the Stern–Volmer equation:

$$\frac{F_0}{F} = 1 + K_{SV} \cdot [Q] \tag{11}$$

where F_0 and F are, respectively, fluorescence intensities in the absence and presence of quencher, K_{SV} is the Stern–Volmer dynamic quenching constant and $[Q]$ is the concentration of the quencher. The equation assumes a linear relationship between F_0/F and [Q] with a slope of K_{SV}. The Stern–Volmer constants express the accessibility of the chromophore to the quencher [37].

Statistical analysis

All data are expressed as mean ± S.E.M. of 6 independent experiments. Statistical calculations were done by Origin 7.0 (OriginLab Corp., USA). The Shapiro–Wilk test was used to ensure normal distributions. Statistical analysis of the results was done with Student–Fischer test. Also, the statistical significance of curves was assessed using statistical Box plots including mean, 5% and 95% Wisker lines, 25 and 75 percentiles, and lower and upper confidence intervals (at α=0.05).

Table 1 Binding constants, number of binding centers per molecule and blue shift of ANS fluorescence emission maximum for binding between ANS and water-soluble carbosilane dendrimers

	$K_b \times 10^{-5}$ $(mol/l)^{-1}$	N (μmol/l)	n	Dendrimer/ ANS	$\Delta\lambda$ (from 520 nm to …)
1	0.7–2.0	1–3	0.1–0.3	~8:1	473±1.9 nm
2	0.6–2.1	3–4	0.3–0.4	~3:1	470±1.7 nm
3	1.0–1.5	8–10	0.8–1.2	~1:1	481±1.4 nm
4	1.0–1.4	7–13	0.7–1.3	~1:1	481±1.2 nm

Results and discussion

Double fluorimetric titration using ANS

An aqueous solution of pure ANS fluoresced weakly in the range 400–600 nm with a maximum at 520 nm; its fluorescence yield in a polar environment is low [38]. Figure 2 shows the results of double fluorimetric titration of ANS and dendrimer **3**. Figure 2a, b show that the

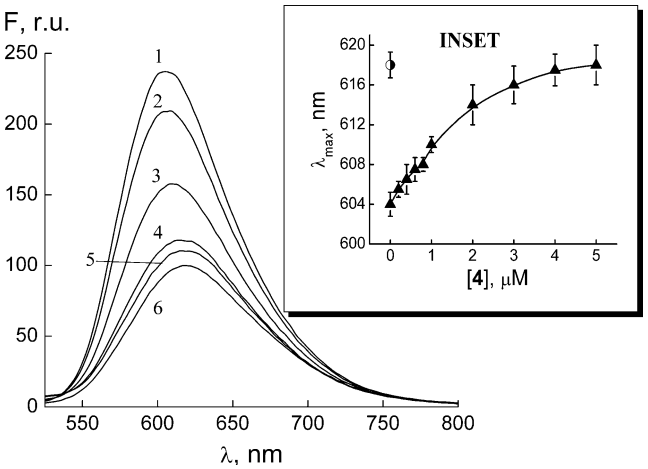

Fig. 3 Fluorescence emission spectra of pure EB (*6*), EB complexed with ctDNA (*1*) and EB–ctDNA complex in the presence of dendrimer **4** at 0.4 μmol/l (*2*), 1 μmol/l (*3*), 2 μmol/l (*4*) and 5 μmol/l (*5*). The spectra at 0.2, 0.6, 3 and 4 μmol/l are not presented. *Inset* shows the dependence of the fluorescence emission maximum of the EB–ctDNA complex on the concentration of dendrimer **4** (*triangles*). The fluorescence emission maximum of pure EB is shown as a *circle*. [EB]=1 μg/ml, [DNA]=3 μg/ml, $\lambda_{ex.}$=477 nm, 0.15 mol/l Na-phosphate buffer, pH 7.4, 37°C

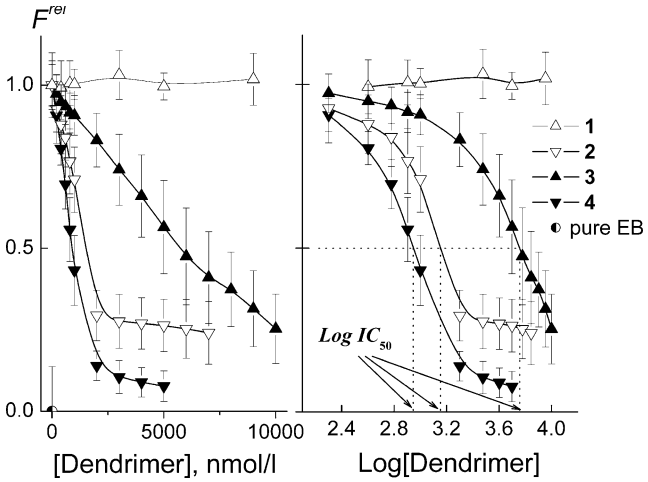

Fig. 4 The displacement of EB from DNA by carbosilane dendrimers. For details see "Materials and methods". [EB]=1 μg/ml (2.54 μmol/l), [DNA]=3 μg/ml, 0.15 mol/l Na-phosphate buffer, pH 7.4, 37°C. $\lambda_{ex.}$=477 nm, $\lambda_{em.}$=604 nm

fluorescence intensity increases non-linearly and reaches a plateau at high dendrimer and ANS concentrations. The Scatchard curve is approximately linear. Table 1 presents the binding constants, the number of binding centers, the approximate ANS:dendrimer molar ratio and the spectral shift in ANS for all the dendrimers studied. Adding carbosilane dendrimers led to both a sharp increase in fluorescence intensity (Fig. 2) and a blue shift of the emission maximum (λ_{max}; Table 1). These changes indicate that ANS interacts with the dendrimers. When the ANS probe is bound to hydrophobic sites in membranes or proteins it fluoresces strongly [39], so the results may suggest that the bound ANS is located in a more hydrophobic environment in the dendrimer. On the other hand, some authors claim that ANS binds to cationic groups in proteins and that its binding depends on ion-pair formation [40]. The binding data show that one molecule of an NN group dendrimer binds one molecule of ANS with a K_b of 10^5. Second generation dendrimers have open, asymmetric structures capable of encapsulating ANS. In contrast, the parameter n ranged from 0.1 to 0.3 for the N group dendrimers, suggesting that micelle formation rather then true molecular binding takes place. In this case, three or ten dendrimer molecules surround one ANS molecule, changing its fluorescence parameters. These data show that the NN group dendrimers bind more effectively than the less reactive N group dendrimers.

Ethidium bromide intercalation assay

EB, a fluorescent phenanthridine dye, is widely used for visualizing nucleic acids [41]. When the dye interacts with nucleic acids its λ_{max} is blue-shifted and its fluorescence intensity is enhanced. It has been confirmed that EB binds to DNA by intercalation [42]. Analytical techniques including circular dichroism, laser flash photolysis, fluorescence and molecular absorption have been used to study the intercalation of EB in DNA [43–45]. The extent of fluorescence quenching of DNA-bound EB has been used to determine the extent of binding between DNA and other ligands such as metal complexes [46], tannic and ellagic acids [47] and cationic polymers [48, 49].

The emission spectra of DNA-bound EB in the absence and presence of dendrimer **4** are shown in Fig. 3. To exclude interactions between EB and dendrimers, it was shown that the dendrimers did not affect the shape or intensity of the EB spectrum even at the highest concentrations used.

The addition of dendrimer to the DNA–EB complex lowered the EB fluorescence emission intensity, indicating that dendrimer **4** competes with EB for DNA binding. The fluorescence emission maximum of free EB was 618 nm and that of the EB–DNA complex was 604 nm. Increasing amounts of **4** caused a concentration-dependent red shift of this maximum from 604 to 618 nm.

Similar results were obtained for all the other dendrimers. In all cases (except for **1**) the EB fluorescence emission intensity was decreased and the EB fluorescence emission maximum was red-shifted. The results show that all the dendrimers bound to DNA and displaced EB from its sites of intercalation (Fig. 4).

On the basis of the results in Fig. 4, the apparent association (binding) constants of three carbosilane dendrimers were calculated using two similar approaches. These constants are given in Table 2.

The data show that **3** had an association constant comparable with that of EB while the interaction of **1** with

Table 2 The association constants of carbosilane dendrimers **2**, **3**, **4** with ctDNA

Dendrimer	LogIC_{50} (see Fig. 4)	IC_{50} (=$[D]_{50}$), μmol/l	$K_{ass}^{DEN} \times 10^{-5}$, $(mol/l)^{-1}$	$K_{ass}^{I} \times 10^{-5}$, $(mol/l)^{-1}$
2	3.16 (3.06–3.26)[a]	1.45 (1.15–1.82)	2.98 (2.38–3.76)	3.67 (2.92–4.62)
3	3.76 (3.6–3.93)[a]	5.75 (3.98–8.51)	0.75 (0.51–1.09)	0.92 (0.62–1.34)
4	2.95 (2.83–3.08)[a]	0.89 (0.68–1.2)	4.85 (3.6–6.36)	5.98 (4.43–7.82)

[a] The upper and lower intervals were obtained from B-splines of two curves (F±SD) vs Log[Dendrimer] in the same manner as for F vs Log [Dendrimer] (see "Materials and methods").

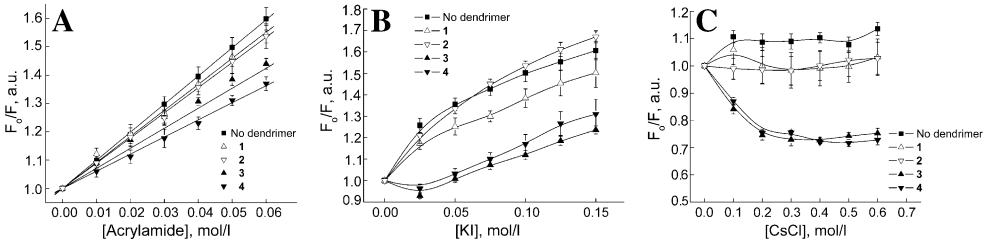

Fig. 5 Curves of BSA fluorescence quenching by acrylamide (**a**), KI (**b**) and CsCl (**c**) in the absence and presence of carbosilane dendrimers. [BSA]=5 μmol/l, [Dendrimer]= 100 μmol/l. $\lambda_{exc.}$=295 nm, $\lambda_{em.}$=350 nm

ctDNA was so weak that it was impossible to estimate its association constant using EB. In contrast, dendrimers with 16 end groups had greater association constants than EB; **4** showed the greatest constant among all the dendrimers studied. This indirect means of determining binding affinity may be misleading, however, because multiple mechanisms for the displacement have been suggested, including conformational changes that modify base stacking and charge repulsion between the dye and polyamine polymers.

Quenching of BSA fluorescence emission in presence of dendrimers

BSA has two tryptophan residues. One is located at the bottom of the hydrophobic pocket in subdomain IIA (Trp^{213}), and the other is on the surface of the molecule in subdomain IB (Trp^{134}) [50]. Three different quenchers, acrylamide, caesium chloride and potassium iodide, were used for experiments on BSA fluorescence quenching in the absence and presence of dendrimers. Acrylamide is a neutral polar quencher that can penetrate the interior of proteins by diffusion because of fluctuations in polypeptide conformation. Both tryptophanyls, Trp^{134} (at the BSA surface) and Trp^{213} (in a hydrophobic pocket), are accessible to acrylamide. Ionic quenchers suppress tryptophan fluorescence by a heavy ion effect, requiring a direct collision between the ions (I^- or Cs^+) and the excited indole ring. Ionic quenchers are not expected to penetrate into the protein matrix, so they can only quench tryptophan residues are located on the protein surface [51]. Because both Trps are accessible to acrylamide the quenching results were analyzed using the Stern–Volmer equation (11).

Figure 5a shows the quenching of BSA fluorescence by acrylamide in the absence and presence of dendrimers. The quenching curves are linear. Quenching was maximal in dendrimer-free media. In the presence of N group dendrimers, the quenching process was close to that in controls. In contrast, the presence of NN group dendrimers decreased the effect of acrylamide. The quenching constants are presented in Table 3. A possible reason is the attachment of NN group dendrimers to the protein surface, generating a layer that restricts the accessibility of the protein to the quencher. N group dendrimers apparently cannot interact effectively with the protein. Figure 5b shows the quenching of BSA fluorescence by the anionic quencher KI in the absence and presence of dendrimer. The data show that the quenching process is complex and quasi-linear; it is non-linear in the initial step (0–0.025 mol/l) but linear over the concentration range 0.025–0.15 mol/l, showing that quenching has both a static and dynamic nature. Collisional quenching is dynamic while the attachment of the quencher to the protein may be static. As for acrylamide, N and NN type dendrimers differ. N group dendrimers affect the quenching process only slightly. In contrast, the addition of NN group dendrimers at initial concentrations sharply decreases the quenching induced by KI. The explanation may be the same as for acrylamide: NN group dendrimers attached to the protein surface prevent any interaction between protein and quencher. Figure 5c shows the quenching of BSA fluorescence emission by CsCl in the absence and presence of dendrimers. As in the case of KI, the quenching process is non-linear. CsCl quenches BSA fluorescence only slightly. Addition of N group dendrimers prevented quenching while addition of NN group dendrimers led to negative quenching, i.e. the fluorescence intensity increased when CsCl was added. The most likely reason for this effect is a direct interaction between the CsCl and the NN group dendrimers.

Thus, the results show first that carbosilane dendrimers can bind small molecules. Secondly, carbosilane dendrimers can interact with DNA and displace EB from it. Thirdly, carbosilane dendrimers can bind to a protein and decrease its accessibility to other molecules. Taking into account that ODN–carbosilane dendrimer complexes do not interact with BSA [30], it can be concluded that NN group carbosilane dendrimers are good candidates for ODN and DNA delivery.

Table 3 The constants of BSA fluorescence quenching by acrylamide in the absence and presence of carbosilane dendrimers

	K_{SV} (Ac), $(mol/l)^{-1}$
No dendrimer	9.92±1.01
1	9.19±0.94
2	8.89±1.1
3	7.07±0.61
4	6.05±0.71

Acknowledgements This work was supported by grant ERA-NET MNT 2007.

References

1. Duncan R, Izzo L (2005) Dendrimer biocompatibility and toxicity. Adv Drug Deliv Rev 57(15):2215–2237. doi:10.1016/j.addr.2005.09.019
2. Svenson S, Tomalia DA (2005) Dendrimers in biomedical applications—reflections on the field. Adv Drug Deliv Rev 57 (15):2106–2129. doi:10.1016/j.addr.2005.09.018
3. Tomalia DA (2004) Birth of a new macromolecular architecture: dendrimers as quantized building blocks for nanoscale synthetic organic chemistry. Aldrichim Acta 37(2):39–57
4. Tomalia DA, Baker H, Dewald J, Hall M, Kallos G, Martin S et al (1986) Dendritic macromolecules: synthesis of starburst dendrimers. Macromolecules 19(9):2466–2468 doi:10.1021/ma00163a029
5. Tomalia DA (1995) Dendrimer molecules. Sci Am 272(5):42–48
6. Ballauff M (2000) Dendrimers III—architecture, nanostructure and supramolecular chemistry. Top. Curr. Chem. 210:177–194
7. Sayed-Sweet Y, Hedstrand DM, Spinder R, Tomalia DA (1997) Hydrophobically modified poly(amidoamine) (PAMAM) dendrimers: their properties at the air–water interface and use as nanoscopic container molecules. J Mater Chem **7**(7):1199–1205. doi:10.1039/a700860k
8. Caminade AM, Laurent R, Majoral JP (2005) Characterization of dendrimers. Adv Drug Deliv Rev 57(15):2130–2146. doi:10.1016/j.addr.2005.09.011
9. Gillies ER, Fréchet JM (2005) Dendrimers and dendritic polymers in drug delivery. Drug Discov. Today 10(1):35–43. doi:10.1016/S1359-6446(04)03276-3
10. Caminade AM, Turrin CO, Sutra P, Majoral JP (2003) Fluorinated dendrimers. Curr Opin Colloid Interface Sci 8(3):282–295. doi:10.1016/S1359-0294(03)00051-7
11. Grayson SM, Jayaraman M, Fréchet JM (1999) Convergent synthesis and 'surface' functionalization of a dendritic analog of polyethylene glycol. Chem Commun Issue 14:1329–1330. doi:10.1039/a902340b
12. Tomalia DA, Berry V, Hall M, Hedstrand DM (1987) Starburst dendrimers. 4. Covalently fixed unimolecular assemblages reminiscent of spheroidal micelles. Macromolecules 20(5):1164–1167. doi:10.1021/ma00171a051
13. Tomalia DA, Naylor AM, Goddard WA III (1990) Starbust dendrimers: molecular-level control of size, shape, surface chemistry, topology, and flexibility from atoms to macroscopic matter. Angew Chem Int Ed Engl 29(2):138–175. doi:10.1002/anie.199001381
14. Tomalia DA, Hall M, Hedstrand DM (1987) Starburst dendrimers. 3. The importance of branch junction symmetry in the development of topological shell molecules. J Am Chem Soc 109 (5):1601–1603. doi:10.1021/ja00239a068
15. Naylor AM, Goddard WA III, Kiefer GE, Tomalia DA (1989) Starburst dendrimers. 5. Molecular shape control. Am Chem Soc 111(6):2339–2341. doi:10.1021/ja00188a079
16. Yang H, Lopina ST (2003) Penicillin V-conjugated PEG-PAMAM star polymers. J Biomater Sci Polym Ed 14:1043–1056. doi:10.1163/156856203769231556
17. Yang H, Lopina ST (2005) Extended release of a novel antidepressant, venlafaxine, based on anionic polyamidoamine dendrimers and poly(ethylene glycol)-containing semi-interpenetrating networks. J Biomed Mater Res 72A:107–114 Part A. doi:10.1002/jbm.a.30220
18. Malik N, Evagorou EG, Duncan R (1999) Dendrimer-platinate: a novel approach to cancer chemotherapy. Anticancer Drugs 10 (8):767–776. doi:10.1097/00001813-199909000-00010
19. Wang D, Kopecek P, Mink T, Nanayakkara V, Kopecek J (2000) Synthesis of starlike N-(2-hydroxypropyl)methacrylamide copolymers: potential drug carriers. Biomacromolecules 1(3):313–319. doi:10.1021/bm0000236
20. Patri AK, Kukowska-Latallo JF, Baker JR (2005) Targeted drug delivery with dendrimers: comparison of the release kinetics of covalently conjugated drug and non-covalent drug inclusion complex. Adv Drug Deliv Rev 57(15):2203–2214. doi:10.1016/j.addr.2005.09.014
21. Zhuo RX, Du B, Lu ZR (1999) In vitro release of 5-fluorouracil with cyclic core dendritic polymer. J. Control. Release 57:249–257. doi:10.1016/S0168-3659(98)00120-5
22. D'Emanuele A, Atwood D (2005) Dendrimer–drug interactions. Adv Drug Deliv Rev 57(15):2147–2162. doi:10.1016/j.addr.2005.09.012
23. Kabanov VA, Zezin AB, Rogacheva VB, Gulyaeva ZG, Zansochova MF, Joosten JGH et al (1999) Interaction of Astramol poly (propyleneimine) dendrimers with linear polyanions. Macromolecules 32:1904–1909. doi:10.1021/ma9716443
24. Li Y, Dubin PL, Spindler R, Tomalia DA (1995) Complex formation between poly(dimethyldiallylammonium chloride) and carboxylated starburst dendrimers. Macromolecules 28:8426–8428. doi:10.1021/ma00128a064
25. Kannan S, Kolhe P, Raykova V, Glibatec M, Kannan RM, Lieh-Lai M et al (2004) Dynamics of cellular entry and drug delivery by dendritic polymers into human lung epithelial carcinoma cells. J Biomater Sci Polym Ed 15:311–330. doi:10.1163/156856204322977201
26. Wiwattanapatapee R, Jee RD, Duncan R, (1999) PAMAM dendrimers as a potential oral drug delivery system: dendrimer complexes with piroxicam. Proc Int Symp Control Release Bioact Mater 145–146 (26th)
27. Chauhan AS, Sridevi S, Chalasani KB, Jain AK, Jain SK, Jain NK et al (2003) Dendrimer-mediated transdermal delivery: enhanced bioavailability of indomethacin. J Control Release 90:335–343. doi:10.1016/S0168-3659(03)00200-1
28. Ortega P, Bermejo JF, Chonco L, de Jesus E, Javier de la Mata F, Fernández G et al (2006) Novel water-soluble carbosilane dendrimers: synthesis and biocompatibility. Eur J Inorg Chem **7**:1388–1396. doi:10.1002/ejic.200500782
29. Bermejo JF, Ortega P, Chonco L, Eritja R, Samaniego R, Müllner M et al (2007) Water-soluble carbosilane dendrimers: synthesis, biocompatibility and complexation with oligonucleotides; evaluation for medical applications. Chem Eur J 13:483–495. doi:10.1002/chem.200600594
30. Chonco L, Bermejo-Martin JF, Ortega P, Shcharbin D, Pedziwiatr E, Klajnert B et al (2007) Water-soluble carbosilane dendrimers protect phosphorothioate oligonucleotides from binding to serum proteins. Org Biomol Chem 5:1886–1893. doi:10.1039/b703989a
31. Shcharbin D, Pedziwiatr E, Chonco L, Bermejo-Martin JF, Ortega P, Javier de la Mata F, Eritja R, Gomez R, Klajnert B, Bryszewska M, Angeles Muñoz-Fernandez M (2007) Analysis of interaction between dendriplexes and bovine serum albumin. Biomacromolecules 8:2059–2062. doi:10.1021/bm070333p
32. Shcharbin D, Klajnert B, Mazhul V, Bryszewska M (2003) Estimation of PAMAM dendrimers' binding capacity by fluorescent probe ANS. J Fluoresc 13(6):519–524. doi:10.1023/B:JOFL.0000008063.28420.45
33. Pang J-Y, Long Y-H, Chen W-H, Jiang Z-H (2007) Amplification of DNA-binding affinities of protoberberine alkaloids by appended polyamines. Bioorg Med Chem Lett 17(4):1018–1021. doi:10.1016/j.bmcl.2006.11.037

34. Cheng YC, Prusoff WH (1973) Relationship between the inhibition constant (K^I) and the concentration of inhibitor which causes 50 per cent inhibition (I_{50}) of an enzymatic reaction. Biochem Pharmacol 22:3099–3108. doi:10.1016/0006-2952(73)90196-2
35. Klotz IM (1985) Ligand–receptor interactions: facts and fantasies. Q Rev Biophys 18:227–259
36. Tang T-C, Huang H-J (1999) Electrochemical Studies of the Intercalation of Ethidium Bromide to DNA. Electroanalysis 11 (16):1185–1190. doi:10.1002/(SICI)1521-4109(199911)11:16<1185::AID-ELAN1185>3.0.CO;2-#
37. Lakowicz JR (1999) Principles of Fluorescence Spectroscopy 2nd ed. Kluwer Academic/Plenum, New York
38. Slavik J (1982) Anilinonaphthalene sulfonate as a probe of membrane composition and function. Biochim Biophys Acta 694(1):1–25
39. Radda GK (1972) Fluorescent probes in membrane studies. Biomembranes 3:247–266
40. Matulis D, Baumann C, Bloomfield V, Lovrien R (1999) 1-Anilino-8-naphthalene sulfonate as a protein conformational tightening agent. Biopolymers 49(6):451–458. doi:10.1002/(SICI)1097-0282(199905)49:6<451::AID-BIP3>3.0.CO;2-6
41. Quillardet P, Hofnung M (1988) Ethidium bromide and safety—readers suggest alternative solutions. Trends Genet 4:89–93. doi:10.1016/0168-9525(88)90092-3
42. Tsai CC, Jain SC, Sobel HM (1977) Visualization of drug–nucleic acid interactions at atomic resolution. I. Structure of an ethidium/dinucleoside monophosphate crystalline complex, ethidium:5-iodouridylyl (3¢-5¢) adenosine. J Mol Biol 114(3):301–315. doi:10.1016/0022-2836(77)90252-2
43. Chen W, Turro NJ, Tomalia DA (2000) Using ethidium bromide to probe the interactions between DNA and dendrimers. Langmuir 16(1):15–19. doi:10.1021/la981429v
44. Pope LH, Davies MC, Laughton CA, Roberts CJ, Tendler SJB, Williams PM (2000) Atomic force microscopy studies of intercalation-induced changes in plasmid DNA tertiary structure. J Microsc 199(1):68–78. doi:10.1046/j.1365-2818.2000.00703.x
45. Lee CY, Ryu H-W, Ko T-S (2001) Binding features of ethidium bromide and their effects on nuclease susceptibility. Bull Korean Chem Soc 22:87–89
46. Zhao GH, Lin HK, Zhu SR, Sun HW, Chen YT (1998) Dinuclear palladium(II) complexes containing two monofunctional [Pd(en)(pyridine)Cl]+ units bridged by Se or S. Synthesis, characterization, cytotoxicity and kinetic studies of DNA-binding. J Inorg Biochem 70:219–226. doi:10.1016/S0162-0134(98)10019-3
47. Labieniec M, Gabryelak T (2006) Interactions of tannic acid and its derivatives (ellagic and gallic acid) with calf thymus DNA and bovine serum albumin using spectroscopic method. J Photochem. Photobiol B 82:72–78. doi:10.1016/j.jphotobiol.2005.09.005
48. Zhou Y, Li Y (2004) Studies of the interactions between poly (diallyldimeythyl ammonium chloride) and DNA spectroscopic methods. Colloids Surfaces A Physicochem Eng Aspects 233:129–135. doi:10.1016/j.colsurfa.2003.11.030
49. Klajnert B, Walach W, Bryszewska M, Dworak A, Shcharbin D (2006) Cytotoxicity, haematotoxicity and genotoxicity of high molecular mass arborescent polyoxyethylene polymers with polyglycidol-block-containing shells. Cell Biol Int 30:248–252. doi:10.1016/j.cellbi.2005.10.026
50. Carter DC, Ho XJ (1994) Structure of serum albumins. Adv Protein Chem 45:153–203. doi:10.1016/S0065-3233(08)60640-3
51. Klajnert B, Stanislawska L, Bryszewska M, Palecz B (2003) Interactions between PAMAM dendrimers and bovine serum albumin. BBA 1648:115–126